ELSEVIER

Thermochimica Acta 247 (1994) 55–64

thermochimica acta

Quantitative measurement of the heat exchange during deformation using an infrared camera

Joachim A. Koenen

Universität Ulm, Abt. Experimentelle Physik, Albert Einstein Allee 11, D-89081 Ulm, Germany

Received 5 June 1993; accepted 15 August 1993

Abstract

The observation of the temperature pattern on the surface of a polymeric sample during stretching using an infrared camera is, after stretching calorimetry, a second method for measuring thermoelastic properties. In order to do this, the thermal image from the IR camera has to be transformed to a temperature image using the calibration of the camera and the emissivity of the material. Studies on the necking process in polycarbonate provide a quantitative evaluation of the produced and exchanged heat. The strength of the heat sources of the neck can be obtained by comparison of the experimentally measured temperature profiles and the temperature profiles calculated with a one-dimensional model of the necking, including heat generation, heat conduction and heat loss. The results are in perfect agreement with the stretching calorimeter results, but very fast experiments are possible and instantaneous signals with spatial and temporal resolution can be obtained.

Keywords: Deformation; Heat exchange; Necking; Polycarbonate; Polymer; Polymeric glass

1. Introduction

It is common to use a stretching calorimeter to measure the thermoelastic properties of materials [1–4]. The advantage of this method is the high sensitivity of measuring heat exchanges during deformation. But the method has a very poor temporal resolution due to the large time constants of the apparatus. Therefore, it is impossible to conduct fast experiments with high strain rates. Our study represents another approach. We observe the sample in the stretching device with an infrared camera [5,6]. The thermal image of the camera is transformed to a temperature image of the surface of the sample. Investigations on the necking process in polycarbonate [7–9],

0040-6031/94/$07.00 © 1994 – Elsevier Science B.V. All rights reserved
SSDI 0040-6031(94)01859-F

where there is a very localized deformation zone, at different deformation speeds cover the range from nearly isothermal to adiabatic stretching. Comparison of the measured temperature pattern and a calculation including heat conduction, heat sources and heat loss leads to the intensity of the heat sources and therefore to the complete energy balance of the necking process.

2. Infrared camera

We use an infrared camera from Inframetrics, type 525 (Fig. 1). The incoming infrared beam passes through a germanium filter, which absorbs the visible and near-infrared part of the radiation. The image is scanned with the aid of a mirror that oscillates sinusoidally in the horizontal plane and moves vertically with a sawtooth-like motion. Zooming in to interesting parts of the sample is possible by changing the amplitude of the two oscillations. A lens focuses the beam on the detector which is held in a liquid nitrogen cooled dewar [10]. The detector is an $Hg_xCd_{1-x}Te$ semiconductor with a small band gap. A value of $x \approx 0.3$ leads to a sensitivity range from 8 to 12 μm [11]. The output of the camera is a standard CCIR video signal (25 frames, 50 fields per second, 625 lines per frane). At the bottom of the image a synthetically created grey-level wedge is added by the infrared camera. The technical data are collected in Table 1.

3. Experimental

The stretching experiments were done in a Zwick 1445 tensile tester with a speed ranging from 0.1 to 1000 mm min^{-1}. We used dogbone-shaped samples (DIN 53455

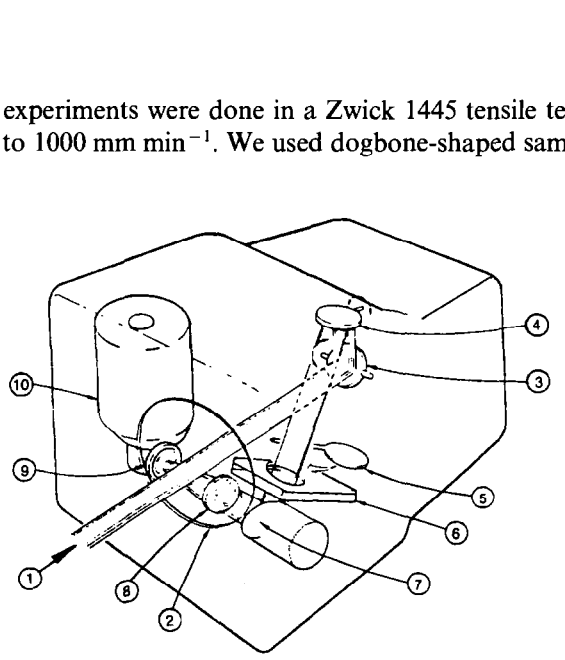

Fig. 1. Sketch of the infrared camera (Inframetrics 525). 1, incoming IR beam; 2, germanium window; 3, vertical scanning mirror; 4, horizontal scanning mirror; 5, shutter; 6, filter support for additional filters; 7, folding mirror; 8, lens focus; 9, window of dewar; 10, detector in dewar.

Table 1
Technical data of the IR camera used

Temperature range	−20°C–1300°C	Zooming range	4:1
Temperature resolution	0.2 K	Time resolution	50 fields, 25 frames per second
Spatial resolution	250 pixel per line	Detector	$Hg_xCd_{1-x}Te$ semiconductor
	200 lines	Output signal	CCIR norm video signal

Nr. 3; size, 100 mm × 10 mm × 4 mm) of polycarbonate of bisphenol A (Makrolon 2800). The sample is observed with the IR camera and a normal video camera to give both an infrared and a normal video, which is used to measure the local strains and the neck velocity (Fig. 2). A third camera points to the force display of the stretching device and a clock is added to the film with a clock and title generator. Therefore all the information, force, strains, time, and IR image, is stored on video (Sony Umatic VO7630 or VO5630). Further evaluation of the experiment is done using an image-processing system plugged into a personal computer (Imaging Technology PFG+).

After digitization, a grey level equalization is performed using a wedge at the bottom of the image, which is synthetically created by the IR camera. This yields a corrected image without intensity-affecting influences on the whole transmission line (cables, image splitters, title/clock generator, recorders, AD converter).

4. Calibration of the infrared camera

To calibrate the whole system from the IR camera to the digitized image on the frame grabber, we have used two black-body radiators at different temperatures. The grey level difference in the intensity image was related to a reference temperature of 20°C (Fig. 3). The solid lines are calculated using the intensity of a black body radiator

$$\rho(T,\lambda) = 2\pi hc^2\lambda^{-5}(e^{hc/k_B T\lambda} - 1)^{-1} \tag{1}$$

(where λ is the wavelength, h Planck's constant, c the speed of light, and k_B Boltzmann's constant), which falls into the sensitive window of the IR camera and can be described by

$$E(\lambda) = \left(\frac{\delta^2}{(\lambda - \lambda_{max})^2 + \delta^2}\right)^2 \tag{2}$$

with $\lambda_{max} = 10\ \mu m$ and $\delta = 4\ \mu m$ [11].

The intensity signal of the IR camera was calculated according to

$$I(T) = G\int_0^\infty E(\lambda)\rho(T,\lambda)\,d\lambda + O \tag{3}$$

with the proportionality constant G and an offset O.

This calculation gives both a good understanding of the measured calibration curves and an excellent interpolation function with which to transform the intensity image into a temperature image.

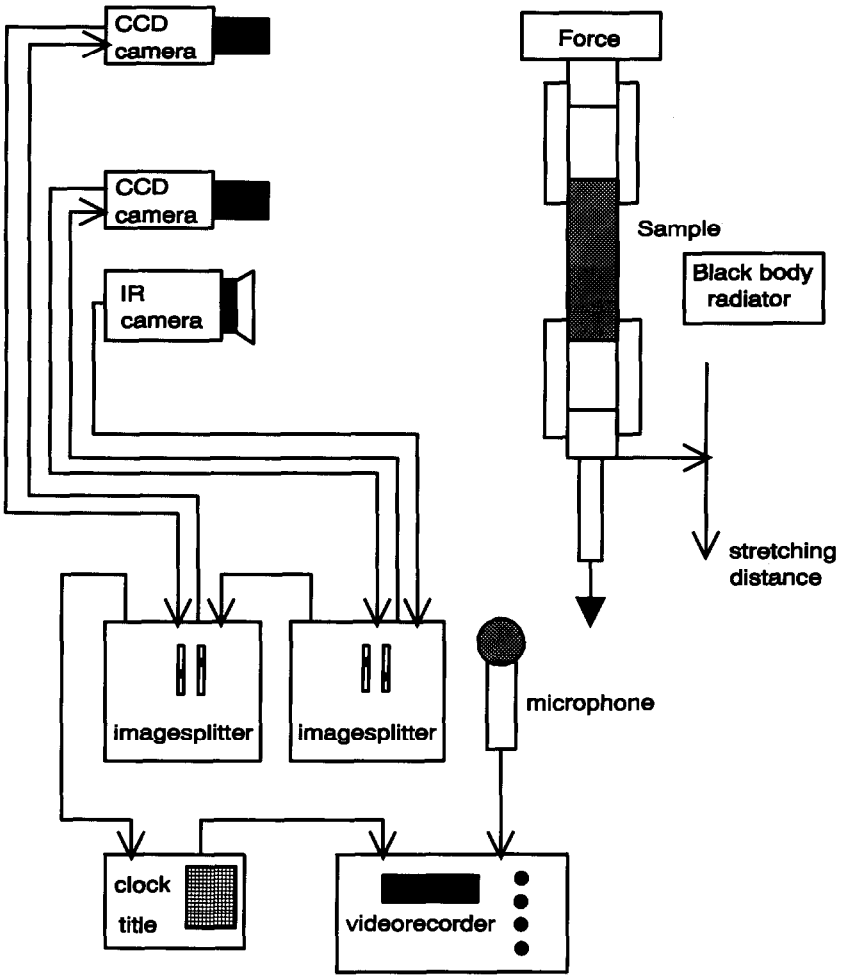

Fig. 2. Experimental setup for measurements with the IR camera during tensile tests and calibration. The IR camera observes the sample and the black-body radiator at a reference temperature. One video camera records the line pattern on the sample to measure the local strains. The neck velocity is obtained by using the clock and the video film. The second video camera films the force display of the tensile tester. Comments and protocol are made via the microphone.

5. Emissivity, and the coefficients of transmission and reflection

We have to measure the emissivity of our material, because the samples are not black-body radiators. We have done this by measuring the coefficients of transmission τ and reflection ρ, and using Eq. (4) to obtain the emissivity ε

$$\varepsilon + \rho + \tau = 1 \tag{4}$$

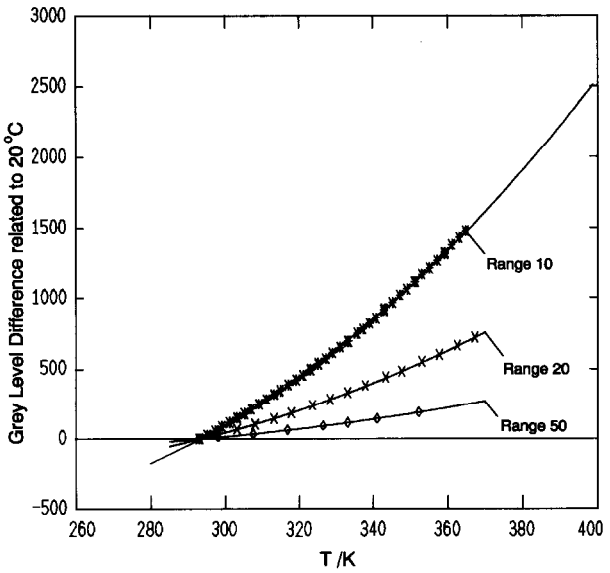

Fig. 3. Calibration of the IR camera at different range selections. The solid lines are calculations with Eq. (3). The grey-level difference related to 20°C is plotted in dependence of temperature.

To obtain τ we observe the light of the black-body radiator with temperature T and intensity $I_{bb}(T)$ transmitted through the sample with intensity I_{sample}. This light is composed of three parts: the transmitted light, the radiation of the sample with $T = T_{sur}$ itself ($I_{bb}(T_{sur})$), and the reflected light of the surroundings with intensity $I_{bb}(T_{sur})$

$$I_{sample} = \tau I_{bb}(T) + \varepsilon I_{bb}(T_{sur}) + \rho I_{bb}(T_{sur}) \tag{5}$$

This yields, with Eq. (4)

$$\tau = \frac{I_{sample} - I_{bb}(T_{sur})}{I_{bb}(T) - I_{bb}(T_{sur})} \tag{6}$$

To obtain ρ, we observe the reflected light of a black-body radiator

$$\rho = \frac{I_{sample} - I_{bb}(T_{sur})}{I_{bb}(T) - I_{bb}(T_{sur})} \tag{7}$$

For polycarbonate, we measured the following values for wavelengths in the range 8–12 μm: $\rho = 0.06$, $\tau = 0.02$ (0.3-mm-thick sample), $\tau = 0$ (1-mm- and 4-mm-thick samples), $\varepsilon = 0.94$ (1-mm- and 4-mm-thick samples).

6. Transformation from thermal to temperature image

The signal of the IR camera on observing an object with $\varepsilon < 1$ consists of three parts: the emitted, the reflected and the transmitted light

$$I_{obj} = \varepsilon I_{bb}(T_{obj}) + \rho I_{bb}(T_{sur}) + \tau I_{bb}(T_{sur}) \quad (8)$$

From calibration, we know the relation between the intensity of a black-body radiator and its temperature. Eqs. (4) and (8) yield

$$I_{bb}(T_{obj}) = (1/\varepsilon) I_{obj} + (1 - \varepsilon) I_{bb}(T_{sur}) \quad (9)$$

With this equation we can calculate the temperature of a sample with emissivity ε in surrounding, of temperature T_{sur}. This is done by the image-processing system.

7. Necking in polycarbonate

Polycarbonate, like other polymers, has a strange deformation behavior. At low strain it obeys Hook's law (Fig. 4). At the yield point, where the nominal stress has a relative maximum, the deformation becomes heterogeneous [7,9,12,13]. A zone

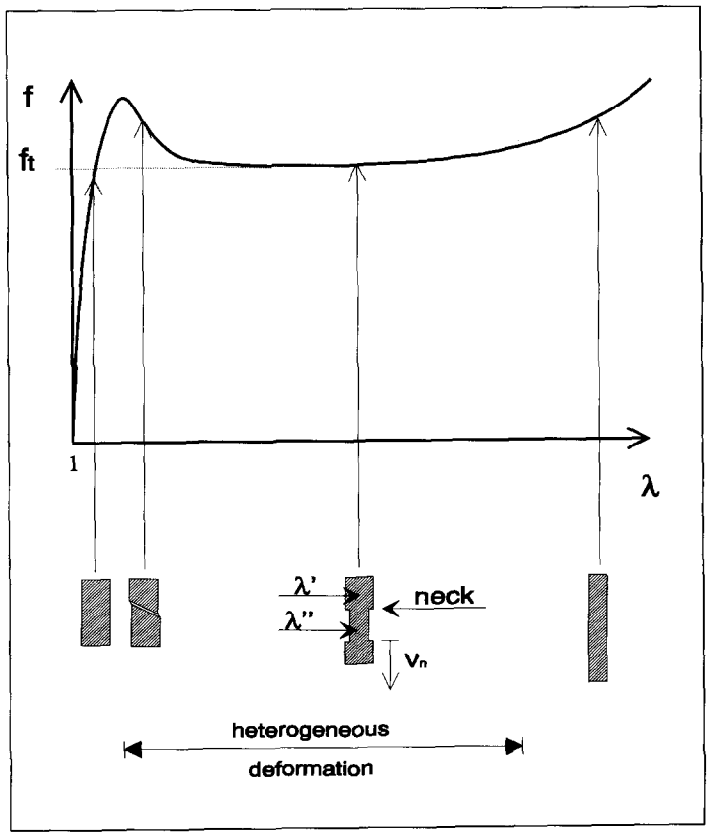

Fig. 4. Schematic stress–strain curve of a polymeric glass showing a yieldpoint and heterogeneous deformation (necking).

with a higher strain λ'' appears on the sample, while the rest has a lower strain λ'. On further stretching, the boundary between the two zones with different strains, called the neck, moves with a constant velocity v_n at a constant nominal stress f_t over the sample. Deformation becomes homogeneous again, when the neck has moved over the entire specimen.

The transition from λ' to λ'' is accompanied by an exchange of mechanical work and heat [8]. The work done per volume can be written

$$w_t = f_t(\lambda'' - \lambda') \tag{10}$$

The heat can be measured with a deformation calorimeter [1,4] or by evaluation of the measured temperature pattern on the sample.

8. Temperature distribution of a neck

We assume a heat source with constant strength at the neck. This heat will disperse according to the law of heat conduction, will be lost at the surface due to heat transfer, and will be transported with the deformation of the material. The one-dimensional differential equation of heat conduction is [14]

$$\frac{\partial^2}{\partial x^2}\vartheta - \frac{1}{\kappa}\frac{\partial}{\partial t}\vartheta = -\frac{A}{K} + \frac{v}{\kappa}\vartheta \tag{11}$$

with t being time, ϑ the temperature difference with the surrounds, ρ_m density, c heat capacity, K heat conductivity, and $\kappa = K/(\rho_m c)$.

On the right of Eq. (11), we have the source term A/K and the loss term with

$$v = \frac{Hp}{c\rho_m \omega} \tag{12}$$

H being the constant of heat transfer, p the perimeter and ω the cross-section.

The necking process is responsible for the heat sources A and we assume an amount of heat q_t per volume being produced. Therefore we get

$$A(x,t) = q_t\,\delta(x - v_n t) \tag{13}$$

where δ is the Dirac delta function.

The last term in Eq. (11) describes the heat loss over the length of the sample, which is proportional to the temperature difference ϑ between sample and surroundings. This holds true for small temperature differences [14].

The solution of this equation for a neck with constant velocity v_n on a sample with infinite length is

$$\vartheta(x,t) = \frac{q_t v_n \sqrt{\kappa}}{2\sqrt{\pi}K}\int_{-\infty}^{\infty} dt'\Theta(t-t')\,e^{-v(t-t')}\frac{1}{\sqrt{t-t'}}\,e^{-(x-v_n t')^2/4\kappa(t-t')} \tag{14}$$

Changing to the neck-comoving frame of reference, $x' = x - v_n t$ yields a stationary solution with no time dependence

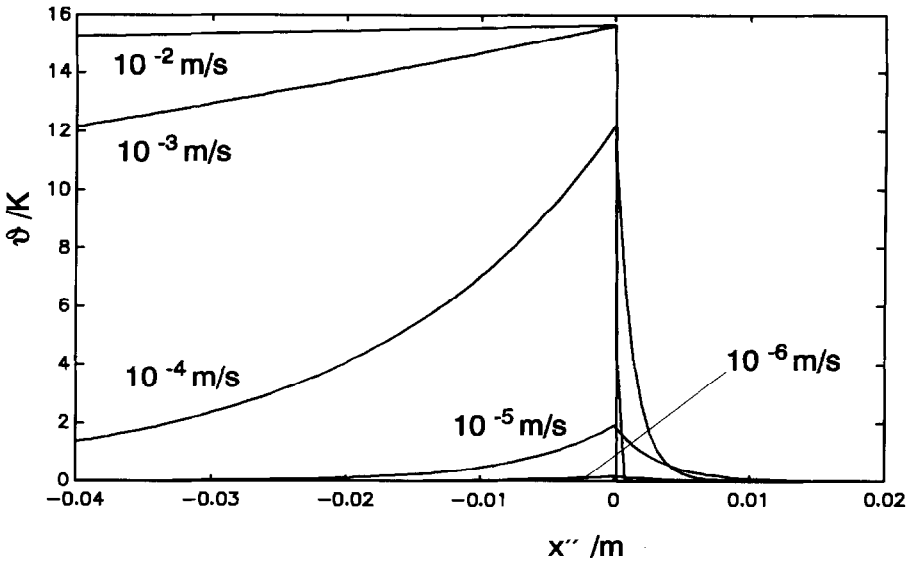

Fig. 5. Temperature profiles calculated theoretically with Eq. (16) for different neck velocities with $q_t = 19$ MPa.

$$\vartheta(x') = \frac{q_t v_n \sqrt{\kappa}}{2\sqrt{\pi K}} \int_{-\infty}^{\infty} d\tau \Theta(\tau)\, e^{-\nu\tau} \frac{1}{\sqrt{\tau}} e^{-(x' + v_n\tau)^2/4\kappa\tau} \tag{15}$$

The material behind the neck transports its heat with the deformation. For our experimentally observed temperature profiles over x'', we have to apply the following transformation

$$x'' = x'\lambda''/\lambda' \qquad \text{if } x' < 0$$

or

$$x'' = x' \qquad \text{under other conditions} \tag{16}$$

In Fig. 5, we see the theoretically calculated temperature profiles with a constant q_t for different v_n.

9. Heat transfer constant

The heat transfer constant ν in Eq. (11) was determined in a Newtonian cooling experiment. The sample was heated homogeneously to a temperature above room temperature and the temporal change of temperature, when brought into air at room temperature, was observed with the IR camera. It obeys an exponential law

$$\vartheta(t) = \vartheta_0\, e^{-\nu t} \tag{17}$$

Experiments with different ϑ_0 and different ratios of perimeter p and crossection ω were carried out and result in $H/(\mathrm{W\,K^{-1}\,mm^{-2}}) = 13.86$ (Eq. (12)).

10. Results and discussion

The agreement between calculated and measured temperature profiles for different stretching speeds and neck velocities, respectively, can be seen in Fig. 6. At low neck velocities, we deform at nearly isothermal conditions, while at the highest speeds the stretching is nearly adiabatic. All parameters, except q_t, were measured independently and are collected in Table 2. Comparison with stretching calorimeter measurements [8] at lower deformation rates yields a value of $q_t/(\mathrm{MPa}) = 18$ for both methods. Also at the higher neck velocities the entire mechanical work of the transition w_t is transferred into heat q_t. Because it is not reasonable to assume a higher heat production than the work done (this may be the case when the material

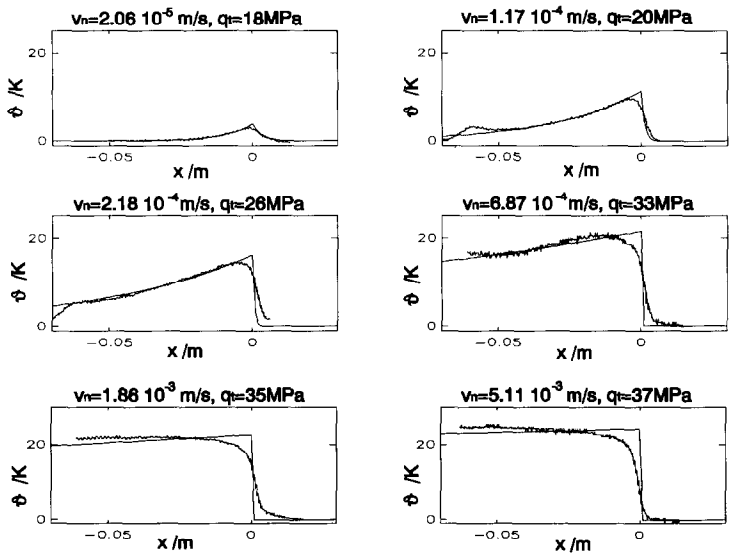

Fig. 6. Measured and calculated temperature profiles of polycarbonate at room temperature at different stretching rates. The parameters are collected in Table 2.

Table 2
Parameters used for calculations

$\varepsilon = 0.94$	$\rho_m = 1.2\ \mathrm{g\,cm^{-3}}$
$\rho = 0.06$	$K = 0.21\ \mathrm{W\,K^{-1}\,m^{-1}}$
$\tau = 0.0$	$H = 13.86\ \mathrm{W\,K^{-1}\,m^{-2}}$
$c = 1.17\ \mathrm{J\,K^{-1}\,g^{-1}}$	

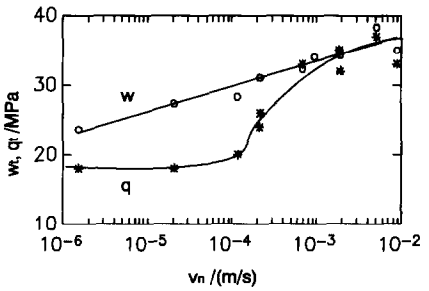

Fig. 7. Work and heat of the transition from state λ' to state λ'' in dependence of the neck velocity.

crystallizes, which is not the case for PC), the quantitative success of the demonstrated method is apparent over the whole range of deformation speeds.

The plot in Fig. 7 shows the mechanical work w_t at the heat q_t in dependence of the logarithm of the neck velocity. At a neck velocity of about 2×10^{-4} m s^{-1}, we see a strong increase of q_t from a constant value at lower v_n until it reaches the work w_t. This behavior may be a relaxation effect or a cooperative process, transforming the entire work into heat at high stretching rates. Therefore, at low neck velocities, the internal energy increases with the transition $\lambda' \rightarrow \lambda''$, while at the highest speeds it remains constant.

The method developed to measure the complete energy balance during tensile tests, is an extension to the measurements in a stretching calorimeter and may be termed 'fast calorimetry'.

References

[1] F.H. Müller and A. Engelter, Kolloid Z., 152 (1957) 15.
[2] H.G. Kilian and G.W.H. Höhne, Thermochim. Acta, 69 (1983) 199.
[3] Y.K. Godovski, Thermophysical Properties of Polymers, Springer, Berlin, 1992.
[4] G.W. Adams and R.J. Farris, J. Polym. Sci. Polym. Phys. Ed., 26 (1988) 433.
[5] J.W. Maher, R.N. Haward and J.N. Hay, J. Polym. Sci. Polym. Phys. Ed., 18 (1980) 2169.
[6] J.A. Koenen, Polymer, 33 (1992) 4732.
[7] R.N. Haward, The Physics of Glassy Polymers, Applied Science Publishers, London, 1973.
[8] J.A. Koenen, H.G. Kilian and B. Heise, J. Polym. Sci. B, Polym. Phys., 27 (1989) 1235.
[9] J.W. Hutchinson and K.W. Neale, J. Mech. Phys. Solids, 31 (1983) 405.
[10] Inframetrics Inc., Bedford, MA, USA, Operations Manual Model 525, 1982.
[11] D. Long and J.L. Schmitt, in R.K. Willardson and A.C. Beer (Eds.), Semiconductors and Semimetals, Vol. 5, Academic Press, New York, 1970.
[12] P.S. Theocaris and C. Hadjiiossiph, Eng. Fract. Mech., 12 (1979) 241.
[13] R.P. Nimmer and L.C. Miller, J. Appl. Mech., 51 (1984) 759.
[14] H.S. Carslaw and J.C. Jaeger, Conduction of Heat in Solids, Clarendon Press, Oxford, 1959.